The Kringle 1 Domain of Hepatocyte Growth Factor Has Antiangiogenic and Antitumor Cell Effects on Hepatocellular Carcinoma

Zan Shen,[1] Zhen Fan Yang,[2] Yi Gao,[1] Ji Cheng Li,[3] Hai Xiao Chen,[4] Ching Chiu Liu,[1] Ronnie T.P. Poon,[2] Sheung Tat Fan,[2] John M. Luk,[2] Kong Hung Sze,[1] Tsai Ping Li,[5] Ren Bao Gan,[5] Ming Liang He,[6] Hsiang Fu Kung,[6] and Marie C.M. Lin[1]

[1]Institute of Molecular Biology, Department of Chemistry and [2]Center for Cancer Research and Department of Surgery, The University of Hong Kong, Pokfulam Road, Hong Kong, China; [3]Institute of Cell Biology, Zhejiang University, Hangzhou, China; [4]Zhejiang Provincial Taizhou Hospital, Zhejiang, China; [5]Institute of Biochemistry and Cell Biology, Shanghai Institute of Biological Sciences, Chinese Academy of Sciences, Shanghai, China; and [6]Stanley Ho Center for Emerging Infectious Diseases, The Chinese University of Hong Kong, Shatin, Hong Kong, China

Abstract

The kringle 1 domain of human hepatocyte growth factor (HGFK1) was previously shown to inhibit bovine aortic endothelial cell proliferation, suggesting that it might be an antiangiogenic molecule. Here, we evaluated the *in vivo* efficacy of a recombinant adenoassociated virus carrying HGFK1 (rAAV-HGFK1) for the treatment of hepatocellular carcinoma (HCC) in a rat orthotopic HCC model and explored its molecular mechanisms *in vitro* in both endothelial and tumor cells. We first showed that rAAV-HGFK1 treatment significantly prolonged the survival time of rats transplanted with tumor cells. Treatment with rAAV-HGFK1 inhibited tumor growth, decreased tumor microvessel density, and completely prevented intrahepatic, lung, and peritoneal metastasis in this *in vivo* model. *In vitro*, rAAV-HGFK1 exhibited both antiangiogenic and antitumor cell effects, inhibiting the proliferation of both murine microvascular endothelial cells (MEC) and tumor cells, and inducing apoptosis and G_0-G_1 phase arrest in these cells. To our surprise, rAAV-HGFK1 did not act through the hepatocyte growth factor/hepatocyte growth factor receptor pathway. Instead, it worked mainly through epidermal growth factor (EGF)/epidermal growth factor receptor (EGFR) signaling, with more minor contributions from vascular endothelial growth factor/vascular endothelial growth factor receptor and β fibroblast growth factor (bFGF)/β fibroblast growth factor receptor (bFGFR) signaling. In both MECs and tumor cells, rAAV-HGFK1 acted through two pathways downstream of EGFR, namely inhibition of extracellular signal-regulated kinase activation and stimulation of p38 mitogen-activated protein kinase/c-Jun-NH_2-kinase activation. These results suggest for the first time that HGFK1 exerts both antiangiogenic and antitumor cell activities mainly through EGF/EGFR signaling, and may thus be considered as a novel therapeutic strategy for the treatment of HCC. [Cancer Res 2008;68(2):404–14]

Introduction

Accumulated evidence has clearly shown that angiogenesis plays an important role in the growth and metastasis of various tumors (1), and antiangiogenic therapy has been shown to be an effective anticancer approach (2–4). Many antiangiogenic molecules have been identified (5), including several kringle domain polypeptides. One of the most well studied kringle domain polypeptides is angiostatin (6), which contains the first four kringles of plasminogen. Each of the angiostatin kringles, as well as the fifth kringle of plasminogen, have been cloned and individually shown to inhibit angiogenesis (7). Similarly, the α-chain of hepatocyte growth factor (HGF), which contains four kringle domains and the NH_2-terminal hairpin domain (NK4), reportedly functions as an antiangiogenic molecule. NK4 has been shown to be bifunctional, as it acts as both an HGF antagonist and an angiogenesis inhibitor (8, 9).

Angiogenesis is critical to the growth and metastasis of hepatocellular carcinoma (HCC), one of the most hypervascular solid tumors (10, 11). The majority of HCC patients present at an advanced stage, and there is no effective systemic treatment currently available for this disease (12–14). Therefore, novel treatment strategies are urgently needed. HCC tissues express higher levels of HGF than dysplastic nodules (15), and high levels of plasma HGF in HCC patients indicate a grave prognosis, suggesting that HGF plays important and active roles in the progression of HCC (16).

We previously found that a recombinant peptide containing the kringle 1 domain of HGF α-chain (HGFK1) inhibits β fibroblast growth factor (bFGF)-stimulated bovine aortic endothelial cell proliferation (17), suggesting that HGFK1 might be an antiangiogenic molecule. However, the *in vivo* efficacy and the molecular mechanisms underlying this effect of HGFK1 have not previously been examined.

A systemic sustained presence is required for an antiangiogenic molecule to achieve an effective anticancer result (18, 19). One strategy for such delivery is the use of gene therapy to direct specific localized synthesis of antiangiogenic polypeptides (20, 21). The adenoassociated virus (AAV) gene therapy vector has been shown to exhibit low pathogenicity and immunogenicity, along with a good ability to transduce growth-arrested cells and produce sustained long-term expression of target genes (22, 23). Here, we examined the use of a recombinant AAV (rAAV) carrying HGFK1 for the *in vivo* treatment of HCC in a rat orthotopic HCC model. We also elucidated the molecular mechanisms of rAAV-HGFK1–mediated antiangiogenic and antitumor cell effects

Note: Supplementary data for this article are available at Cancer Research Online (http://cancerres.aacrjournals.org/).

Requests for reprints: Dr. Marie C.M. Lin, Institute of Molecular Biology, Department of Chemistry, 8/F Kadoorie Biological Science Building, The University of Hong Kong, Pokfulam Road, Hong Kong. Phone: 852-22990776; Fax: 852-28171006; E-mail: mcllin@hkusua.hku.hk.

doi:10.1158/0008-5472.CAN-07-2081

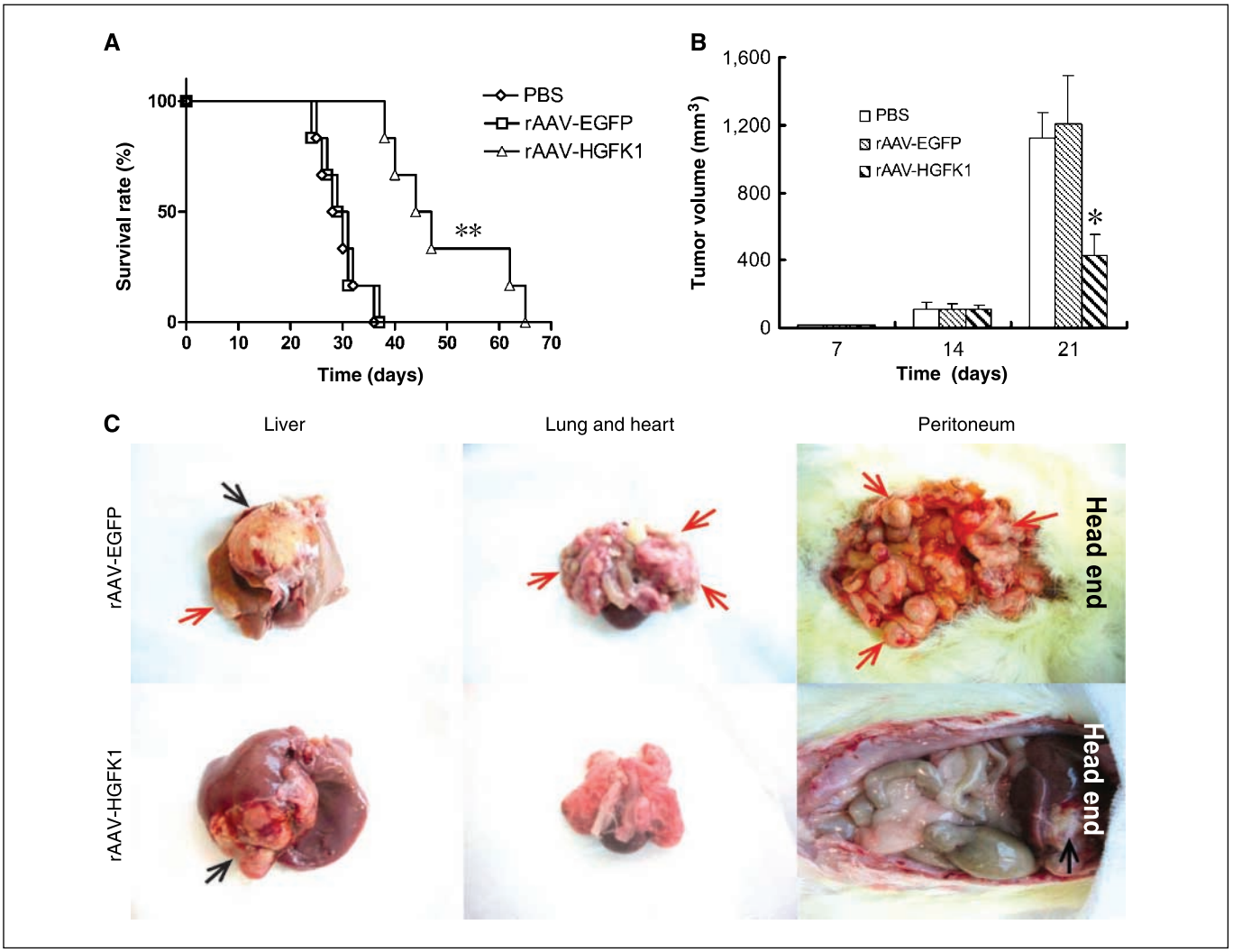

Figure 1. The *in vivo* effects of rAAV-HGFK1 treatment on a rat orthotopic HCC model. Rats received PBS, rAAV-EGFP, or rAAV-HGFK1 by a combination of portal vein and intratumoral injection, as described in Materials and Methods. *A,* survival curves of HCC-bearing rats. **, $P < 0.001$ compared with the PBS-treated group. *B,* tumor volumes. *, $P < 0.01$ compared with the PBS-treated group. *C,* metastasis to the liver, lung, and peritoneum observed at time of death. *Black arrow,* primary tumor. *Red arrow,* metastasis.

in vitro in both murine microvascular endothelial cells (MEC) and rat HCC cells. Finally, we evaluated the possible toxicity of rAAV-HGFK1.

Materials and Methods

Cell culture and materials. The rat HCC cell line, McA-RH7777, the murine tumor-derived MEC line, SVEC4-10EE2, and HEK 293-FT cells were obtained from the American Type Culture Collection. DMEM, fetal bovine serum (FBS), and trypsin-EDTA were purchased from Invitrogen. Cells were maintained as monolayer cultures in DMEM supplemented with 10% FBS (complete DMEM) at 37°C, 5% CO_2.

Because antihuman HGFK1 antibodies were not commercially available, we designed a synthetic peptide corresponding to the NH_2-terminal amino acids of HGFK1 (RSY KGT VSI TKS GIKC) and used this peptide to produce rabbit polyclonal antisera against HGFK1. The polyclonal antibody against CD31 was obtained from PharMingen. The antibodies against epidermal growth factor receptor (EGFR), phosporylated EGFR (P-EGFR), c-Met (HGF receptor), phosphorylated c-Met (P-c-Met), P-Flg, Flk-1 [vascular endothelial growth factor (VEGF) receptor 2], P-Flk-1, Akt, phosporylated Akt, extracellular signal-regulated kinase (ERK), phosphorylated ERK (P-ERK), p38 mitogen-activated protein kinase (MAPK), phosphorylated p38 (P-p38) MAPK, c-Jun NH_2-terminal kinase (JNK), phosphorylated JNK (P-JNK), and β-Actin were purchased from Santa Cruz Biotechnology. The antibodies against Flg (bFGF receptor), caspase 3, cleaved caspapse 3, caspase 9, and cleaved caspase 9 were acquired from Cell Signaling Technology. The specific p38 MAPK inhibitor, SB203580, was purchased from Calbiochem-Novabiochem Corp. The specific JNK kinase inhibitor, SP600125, was purchased from Merck. The EGFR-specific inhibitor, AG1478, was acquired from Sigma-Aldrich. The siRNA against EGFR (si-EGFR) was purchased from Tech Dragon Ltd.

Preparation of rAAV vectors. Plasmids pAAV-CAG-sec-enhanced green fluorescent protein (EGFP) and pAAV-CAG-sec-HGFK1 (Supplementary Data 1) were constructed by inserting fragments encoding the EGFP and human HGFK1 cDNAs into the multiple cloning site of the AAV2 vector [ITR-CAG promoter-Igk leader-EGFP/HGFK1 cDNA-woodchuck posttranscriptional regulatory element (WPRE)-BGH polyA-ITR]. A helper virus-free system was used to produce rAAV particles, as described elsewhere (24, 25), with minor modifications. Briefly, rAAV vectors and the pDG helper plasmid were cotransfected into HEK 293-FT cells by calcium phosphate precipitation. Sixty hours after transfection, cells were trypsinized and resuspended in Tris buffer (pH 8.0). After two cycles of freezing and

thawing, the cells were centrifuged for 20 min at 12,000 rpm and the supernatant containing rAAV-HGFK1 or rAAV-EGFP particles was decanted. The rAAV particles were purified by HiTrap Heparin column chromatography (Sigma). Peak virus fractions were collected and dialyzed against PBS containing 1 mmol/L $MgSO_4$. Samples were then concentrated using a 100K-MicroSep Centrifugal Concentrator (Life Technologies). The viral titer was quantified by real-time PCR, using the Taqman Universal PCR kit (Applied Biosystems) and WPRE-specific primers (forward, 5′-CGG CTG TTG GGC ACT GA-3′; reverse, 5′-CCG AAG GGA CGA AGC AGA AG-3′). Aliquots of each viral stock [2×10^{12} virus genome (vg)/mL] were stored at −80°C before use. A second rAAV vector prepared by AGTC Gene Technology Company Ltd. was tested in parallel in the present study. Both rAAV preparations showed similar efficacies without noticeable toxicity.

Orthotopic HCC model in rats. Male Buffalo rats, 8 to 12 weeks old, weighing 250 to 320 g, were purchased from Charles River Laboratories. All animal experiments were approved in advance by the Committee on the Use of Live Animals in Teaching and Research (University of Hong Kong). The tumor model was induced by injection of 6×10^5 McA-RH7777 cells

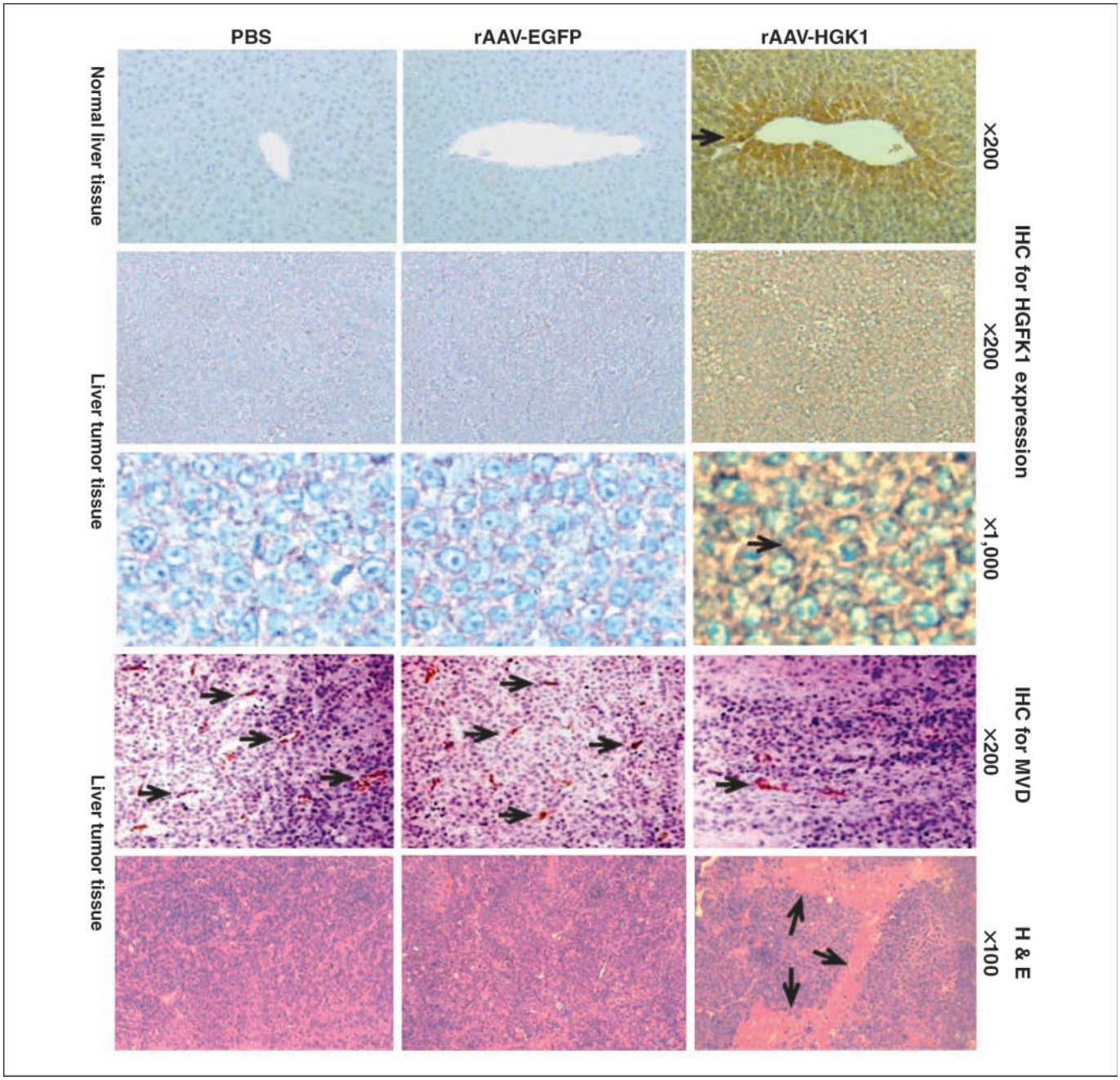

Figure 2. Histologic studies of normal liver and tumor tissues. Rats were treated with PBS, rAAV-EGFP, or rAAV-HGFK1, using a combination of portal vein and intratumoral injections, as described in Materials and Methods. On day 21 posttreatment, rats were sacrificed and tissues were fixed for immunohistochemical (*IHC*) and H&E staining. *Top and second rows*, IHC staining for HGFK1 protein expression (*brown staining*) in normal liver tissues and tumor tissues. *Arrow,* HGFK1-positive cells around a blood vessel. Magnification, ×200. *Third row,* IHC staining of tumor tissues at higher magnification (×1,000). Positive HGFK1 protein expression was observed in the cytoplasm of tumor cells. *Fourth row,* MVD was assessed by immunohistochemical of CD31. Fewer CD31-positive cells were detected in the tumor tissues of rAAV-HGFK1–treated rats compared with the other groups. *Arrows,* CD31-positive cells. Magnification, ×200. *Bottom row,* H&E staining shows that rAAV-HGFK1 but not PBS or rAAV-EGFP treatment is associated with extensive areas of tumor tissue necrosis. Magnification, ×100.

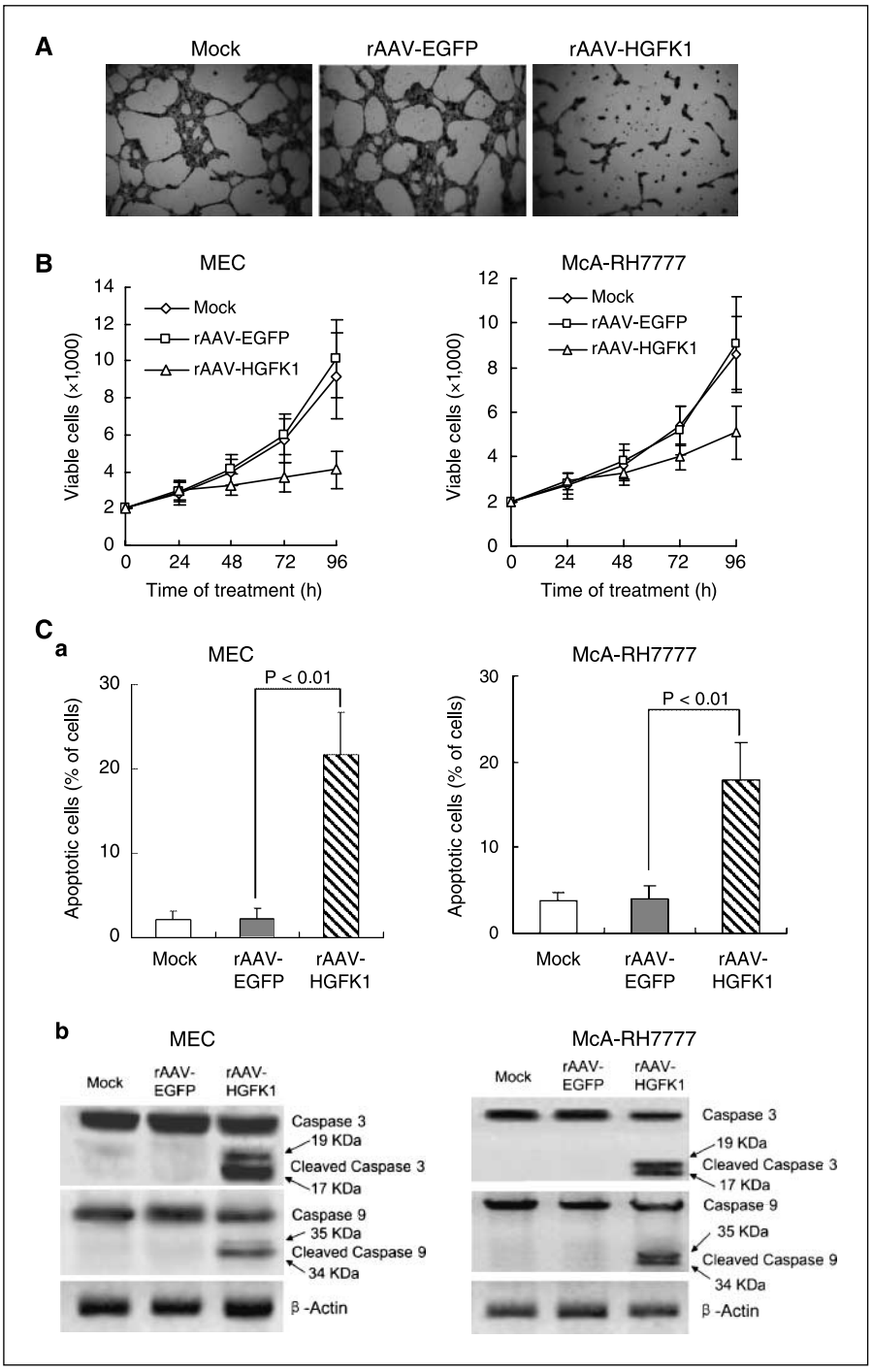

Figure 3. The effects of rAAV-HGFK1 infection on MECs and McA-RH7777 cells. *A, in vitro* angiogenesis assay. Cells were treated with PBS (mock), rAAV-EGFP (MOI, 1×10^4), or rAAV-HGFK1 (MOI, 1×10^4) and incubated in DMEM containing 2% FBS for 48 h. Cells were then seeded (4×10^4 cells per well) in ECMatix gel, and capillary structure formation was observed after 5 h. Magnification, ×100. *B,* cells were seeded in 96-well plates at a density of 2×10^3 cells per well, treated with PBS (*mock*), rAAV-EGFP, or rAAV-HGFK1 (MOI, 1×10^4) and incubated for various time periods in DMEM containing 2% FBS. *Mock,* PBS-treated cells were used as a control. Viable cells were identified by trypan blue exclusion and were counted. *C* and *D,* cells were treated with PBS (mock), rAAV-EGFP, or rAAV-HGFK1 (MOI, 1×10^4) and incubated for 48 h in DMEM containing 2% FBS. *C,* at the end of the incubation, apoptotic cells were stained using the APOPercentage assay kit, and red-stained cells were counted as % of total cells. (*a*). At the end of the incubation, total cellular proteins were extracted and the levels of caspase 3, cleaved caspase 3, caspase 9, and cleaved caspase 9 were analyzed by Western blot (*b*).

into the left lobe of the liver, as described previously (26). Seven days after tumor cell injection, the formation of tumor nodules was confirmed by laparotomy. Each rat developed a single tumor nodule, ranging in size from 3×3 to 3×4 mm^2. The animals were randomly divided into the following groups: (*a*) PBS (nontreatment, $n = 15$); (*b*) rAAV-EGFP ($n = 15$); (*c*) rAAV-HGFK1 ($n = 15$). To achieve a high virus concentration in the tumor tissues and to prevent tumor cells from spreading from tumor tissues to adjacent nontumorous tissues, injections were conducted both intratumorally, at three sites around the margin of tumor nodule, and one site in the center of the tumor nodule (total 0.2×10^{12} vg for the four sites), and also through the portal vein (1×10^{12} vg/rat). The injected volume of vectors or PBS was kept ≤300 μL per rat. Six animals in each group were kept for the survival study, whereas the remaining 9 rats in each group were sacrificed on days 7, 14, and 21 after treatment ($n = 3$ per time point). Immediately after sacrifice, animals were dissected for collection of tumor tissues and organs, including livers and lungs.

Plasma levels of HGFK1. To evaluate long-term rAAV-mediated HGFK1 expression in the circulation, 15 rats were divided into 5 groups ($n = 3$ in each group) and given rAAV-HGFK1 at therapeutic dosage (1.2×10^{12} vg/rat) via injection through the portal vein. On days 0, 7, 21, 60, and 120 postinjection, plasma samples were collected and concentrated, and levels of HGFK1 were measured by Western blot analysis.

Histologic study. Normal and tumor tissues were fixed in 10% buffered formalin and embedded in paraffin. The paraffin-embedded tissues were cut

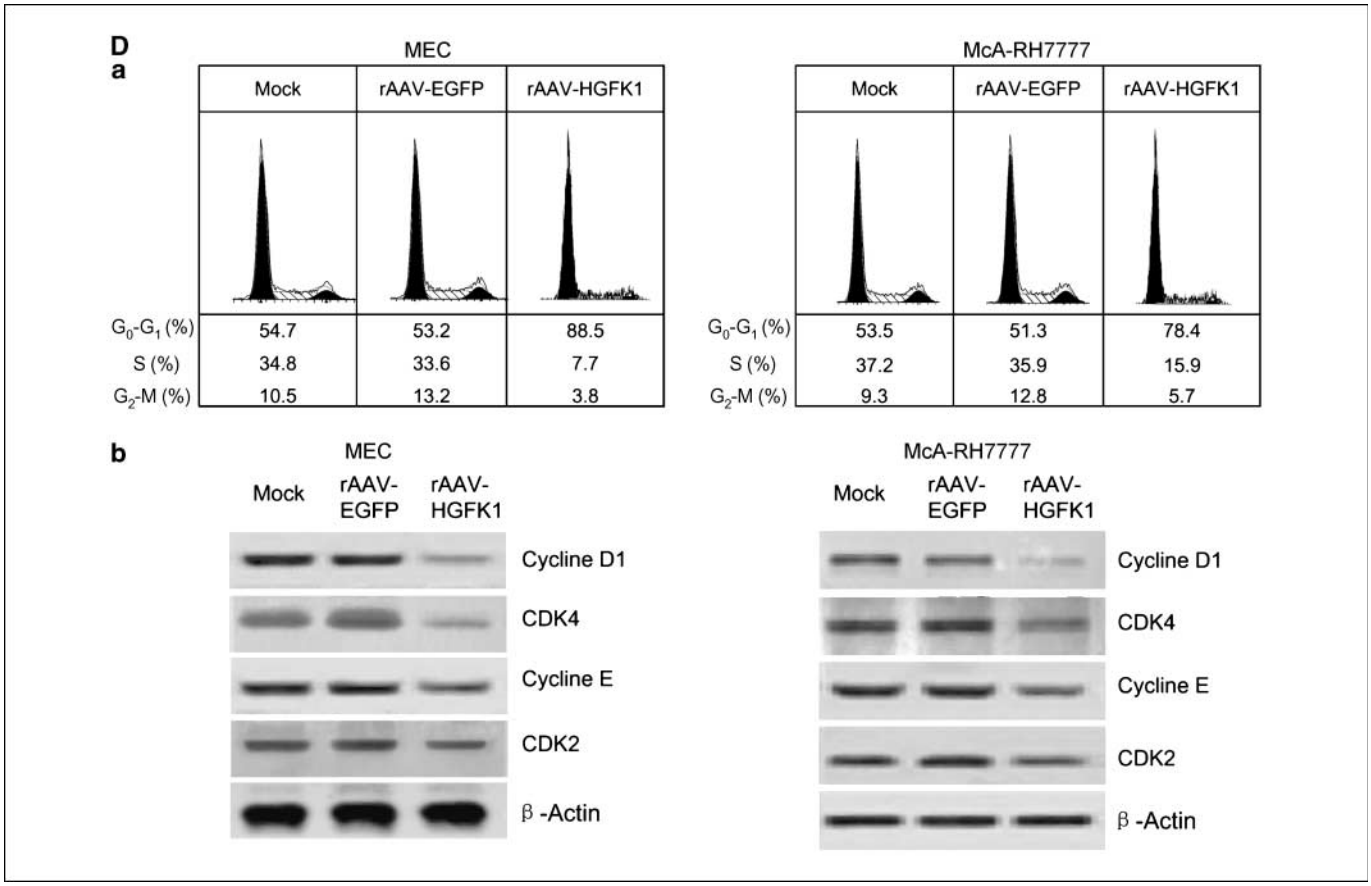

Figure 3 *Continued. D,* cell cycle analysis by flow cytometry revealed that rAAV-HGFK1 treatment was associated with increased G_0-G_1 cell cycle arrest (*a*). Western blot analysis showed that rAAV-HGFK1 treatment led to down-regulation of cyclins and CDKs (*b*). The data shown are representative of the results from three independent experiments.

into 5-μm thick sections and subjected to H&E and immunohistochemical staining, as previously described (27).

Toxicity test. Nine rats (three groups, $n = 3$ per group) were given intraportal vein injections of PBS, rAAV-EGFP (4.8×10^{12} vg/rat), or rAAV-HGFK1 (4.8×10^{12} vg/rat). Body weight and general condition were assessed daily for any signs of systemic toxicity. On days 7 and 60 postinjection, plasma samples were collected for testing of liver biochemistry, including alanine transaminase, aspartate aminotransferase, and total bilirubin levels, as well as cardiac biochemistry, including hydroxybutyric dehydrogenase, creatine kinase, and lactate dehydrogenase levels. The plasma levels of alanine transaminase, aspartate aminotransferase, total bilirubin, hydroxybutyric dehydrogenase, creatine kinase, and lactate dehydrogenase were tested in the clinical biochemistry laboratory of the Queen Mary Hospital (University of Hong Kong). On day 120, animals were sacrificed, and liver and heart tissues were collected. HGFK1 expression was measured by immunohistochemical staining, apoptosis was detected by terminal deoxynucleotidyl transferase-mediated dUTP-biotin end labeling assay, and tissue injury was assessed by H&E staining.

***In vitro* angiogenesis assay.** MECs were seeded in complete DMEM at a density of 3×10^5 cells per well in 6-well plates and allowed to adhere overnight. Cells were then transfected with PBS (mock), or rAAV-EGFP or rAAV-HGFK1 at a multiplicity of infection (MOI) of 1×10^4, and incubated in DMEM with 2% FBS for 48 h. Thereafter, the effect of rAAV-HGFK1 on the angiogenic activity of MECs was evaluated using an *in vitro* angiogenesis assay kit (Chemicon). Briefly, the provided ECMatix was fitted into the wells of a 96-well plate in accordance with the manufacturer's instructions. The transfected MECs were starved for 48 h in DMEM with 0.5% FBS and seeded onto the ECMatix gel (4×10^4 cells per well). Starved nontransfected MECs were seeded in parallel as a control. To assess inhibition of EGFR-specific angiogenesis, cells were treated with PBS (mock), AG1478 (1 μmol/L), or rAAV-HGFK1 (MOI, 1×10^4) and incubated in DMEM with 0.5% FBS for 48 h, and then seeded (4×10^4 cells per well) to plates containing the ECMatix gel. All cells seeded onto the ECMatix gel were incubated for 5 h. Thereafter, the formation of capillary-like structures was inspected using an inverted light microscope (magnification, ×100), and representative fields were photographed.

Cell proliferation assay. McA-RH7777 and MECs were seeded at a density of 2×10^3 cells per well in 96-well plates and allowed to adhere overnight. After adhesion, cells were treated with rAAV-EGFP or rAAV-HGFK1 (MOI, 1×10^4) and incubated for 24, 48, 72, or 96 h in DMEM with 2% FBS. For analysis of growth hormone–stimulated cell proliferation, cells were treated with various MOIs of rAAV-HGFK1, incubated in DMEM with 0.5% FBS for 48 h, and then stimulated with different growth factors in DMEM with 0.5% FBS for an additional 24 h. Cell viability was assessed by trypan blue exclusion, and viable cells were counted manually. All experiments were done in triplicate.

Apoptosis and caspase assays. For our *in vitro* apoptosis assay, McA-RH7777 cells and MECs were seeded in complete DMEM at a density of 2×10^3 cells per well in 96-well plates and allowed to adhere overnight. The cells were then treated with PBS (mock), rAAV-EGFP, or rAAV-HGFK1 (MOI, 1×10^4), and incubated in DMEM containing 2% FBS for 48 h. For our *in vitro* apoptosis assay of cells treated with si-EGFR or AG1478, cells were treated these constructs, incubated in DMEM with 0.5% FBS for 48 h, and then stimulated with epidermal growth factor (EGF; 10 ng/mL) in DMEM with 0.5% FBS for an additional 24 h. The APOPercentage (Biocolor) *in vitro* apoptosis assay kit was used to quantify the number of apoptotic cells. Briefly, 30 min before the end of stimulation, 5 μL of APOPercentage dye was added to each well. At the end of the incubation, the cells were washed

with PBS and the number of apoptotic (red stained) cells was counted under an inverted light microscope at ×400 magnification. Five fields were randomly chosen for each sample.

For analysis of caspase levels and caspase cleavage, cells were seeded in complete DMEM at a density of 3×10^5 cells per well in 6-well plates and allowed to adhere overnight. Cells were then treated as described above, and total proteins were extracted for western blot analysis.

Cell cycle analysis. McA-RH-7777 cells and MECs were seeded in complete DMEM at a density of 3×10^5 cells per well in 6-well plates and allowed to adhere overnight. The cells were then treated with PBS (mock), rAAV-EGFP, or rAAV-HGFK1 (MOI, 1×10^4) and incubated in DMEM with 2% FBS for 48 h. For cell cycle assay of EGF-stimulated cells, cells were treated with PBS (mock), rAAV-EGFP, or rAAV-HGFK1 (MOI, 1×10^4) in DMEM with 0.5% FBS for 48 h and then incubated in DMEM with 0.5% FBS in the presence of 10 ng/mL EGF for 24 h. At the end of the incubations, cells were harvested, washed once with PBS, fixed in citrate buffer (pH 7.6) for 1 h, and resuspended in PBS containing 20 μg/mL of propidium iodide (Calbiochem-Novabiochem Corp.). After a 30-min incubation at 37°C, the cells were subjected to flow cytometric analysis on a FACScan instrument (Becton Dickinson).

Western blot. For Western blot analysis, samples were homogenized in a buffer (pH 7.9) containing 10 mmol/L HEPES, 10 mmol/L KCl, 1.5 mmol/L $MgCl_2$, 0.5 mmol/L DTT, 0.5 mmol/L phenylmethylsulfonyl fluoride, 10 μg/mL aprotinin, and 10 μg/mL leupeptin. The resulting protein extracts were subjected to SDS-PAGE and transferred to a polyvinylidene difluoride membrane. The membrane was incubated with primary and secondary antibodies (1 h each) at room temperature. Signals were developed using an enhanced chemiluminescence kit (Amersham Pharmacia Biotech, Inc.).

siRNA transfection. McA-RH-7777 cells and MECs were seeded at a density of 2×10^4 cells per well in 96-well plates for the proliferation assay and at a density of 3×10^4 cells per well for the apoptosis assay. Cells were transfected with the indicated siRNA according to the different study designs, using Lipofectamine 2000 (Invitrogen Life Technologies; ref. 28). The sequences of the used siRNA are listed in Supplementary Data 2.

Statistical analysis. Animal survival was analyzed by log-rank test using the GraphPad Prism software (GraphPad Software, Inc.). Comparisons of plasma biochemistry variables and numbers of apoptotic cells were carried out using the two-tailed Student's *t* test application of MS Excel. *P* value of <0.05 was considered statistically significant.

Results

rAAV-HGFK1 treatment significantly prolongs survival, inhibits tumor growth, and prevents metastasis in a rat model of HCC. Tumor-bearing rats were established, randomly divided into three groups, and treated with PBS, rAAV-EGFP, or rAAV-HGFK1 (n = 15 per group) by a combination of intratumoral and portal vein injections, as described in Materials and Methods. The results showed that although the median survival time in the control (PBS and rAAV-EGFP) treatment groups were 29 days posttreatment, rAAV-HGFK1 treatment significantly prolonged the median survival time to 49 days ($P < 0.001$; Fig. 1*A*). Furthermore, rAAV-HGFK1 treatment remarkably inhibited tumor growth; the mean tumor size in the rAAV-HGFK1–treated group was significantly smaller than that in the PBS- and rAAV-EGFP–treated groups ($P < 0.01$) on day 21 posttreatment (Fig. 1*B*).

Liver, lung, and peritoneal metastasis was evaluated in all three groups immediately after the animals died. Rats in the PBS (data not shown) and rAAV-EGFP–treated groups (Fig. 1*C, top*) displayed multiple metastatic tumor nodules on the surfaces of the liver, lung, and peritoneum. In contrast, there was no sign of metastasis in members of the rAAV-HGFK1 treatment group (Fig. 1*C, bottom*). In summary (Supplementary Data 3), our results indicate that rAAV-HGFK1 treatment significantly inhibited tumor growth, prevented liver, lung and peritoneal metastasis, and inhibited the accumulation of ascites. In contrast, members of the rAAV-EGFP– and PBS-treated groups displayed 100% liver and peritoneal metastasis, and 100% and 83.3% lung metastasis, respectively.

rAAV-HGFK1 treatment produces sustained high-level HGFK1 expression, resulting in reduced microvessel density and increased tumor tissue necrosis in a rat model of HCC. Immunohistochemical analysis showed that rAAV-HGFK1 treatment produced long-term, high-level HGFK1 protein expression in both normal and tumor tissues in the rats. On day 21 posttreatment, strong HGFK1 protein expression was found in normal liver tissue sections, especially in cells around the blood vessels, in the rAAV-HGFK1 treatment group, but not in the PBS- or rAAV-EGFP–treated groups. HGFK1 protein expression was also found in the primary liver tumor tissues of rAAV-HGFK1–treated rats but not in those of the PBS- or rAAV-EGFP–treated animals (Fig. 2). Nontumor-bearing rats treated with therapeutic doses of rAAV-HGFK1 showed long-term plasma expression of HGFK1 (Supplementary Data 4). Moreover, at a higher magnification (×1,000), it was clear that the HGFK1 protein was expressed mainly in the cytoplasma of liver cells. CD31-specific immunohistochemical staining also showed a significantly lower level of microvessel density (MVD, 6.2 ± 1.6) in the liver tumor tissues of the rAAV-HGFK1 treatment group, compared with sections from the PBS- and rAAV-EGFP–treated groups (25.1 ± 2.1 and 26.8 ± 2.5, respectively; $P < 0.01$). Furthermore, H&E staining showed that rAAV-HGFK1 treatment induced large areas of necrosis in the tumor tissues, whereas only minimal areas of necrosis were observed in tumor tissues from the control groups (Fig. 2).

***In vivo* toxicity test.** The potential toxicity of rAAV-HGFK1 treatment was examined in normal Buffalo rats by portal vein injection of PBS, or a high dosage (4.8×10^{12} vg/rat) of rAAV-EGFP or rAAV-HGFK1 (n = 3 per group). Toxicity was evaluated based on plasma levels of alanine transaminase, aspartate aminotransferase, total bilirubin, hydroxybutyric dehydrogenase, creatine kinase, and lactate dehydrogenase. Our results showed that on days 7 and 60 posttreatment, the plasma levels of alanine transaminase, aspartate aminotransferase, total bilirubin, hydroxybutyric dehydrogenase, creatine kinase, and lactate dehydrogenase were within the reference range in rats from all three groups. Immunohistochemical staining confirmed high-level expression of HGFK1 in liver sections from rAAV-HGFK1–treated rats sampled throughout the treatment period. On day 120 posttreatment, HGFK1 protein expression was still readily detectable by immunohistochemical staining in rAAV-HGFK1–treated rats, whereas no positive HGFK1 signal was found in liver tissues from rats treated with PBS or rAAV-EGFP. Finally, H&E staining showed no detectable injury in the liver and cardiac muscle tissue of rats treated with rAAV-HGFK1 (Supplementary Data 5).

rAAV-HGFK1 inhibits proliferation and induces apoptosis and G_0-G_1 phase arrest in both MECs and tumor cells. We next used cell culture systems to investigate the function of rAAV-HGFK1. We first observed the infection efficacy of the rAAV we constructed for this study and found that rAAV-EGFP could efficiently transduce both MECs and McA-RH7777 cells. Maximum fluorescence was observed in MECs and McA-RH7777 cells (52% and 86% of cells positive, respectively) at 48 h after infection with rAAV-EGFP (MOI, 1×10^4). Western blot analysis detected HGFK1 protein in cell lysates and culture media from both cell types by

48 h after infection with rAAV-HGFK1 (MOI, 1×10^4; Supplementary Data 6).

In vitro angiogenesis assays were then performed to verify the antiangiogenic effect of rAAV-HGFK1. Our results showed that treatment with rAAV-HGFK1 (MOI, 1×10^4) inhibited the ability of MECs to form capillary-like structures (Fig. 3*A*). To further test whether rAAV-HGFK1 exhibited both antiangiogenic and antitumor cell effects, we examined the effect of our construct on both MECs and McA-RH7777 cells. Treatment with rAAV-HGFK1 (MOI, 1×10^4) inhibited the proliferation of both MECs and McA-RH7777 cells (Fig. 3*B*) and induced apoptosis in these cells, as determined by an *in vitro* apoptosis assay and caspase assays (Fig. 3*C*). In addition, flow cytometric cell cycle analysis revealed that rAAV-HGFK1 treatment triggered G_0-G_1 phase arrest, as verified by observation of down-regulated cyclin and cyclin-dependent kinase (CDK) expression in both MECs and tumor cells treated with our construct (Fig. 3*D*).

rAAV-HGFK1 inhibits the activation of EGFR, VEGFR, and bFGFR but not HGFR. We then investigated which receptor rAAV-HGFK1 used to transduce its signal. Specifically, we examined the effect of rAAV-HGFK1 on HGF-, EGF-, VEGF- and bFGF-stimulated cell proliferation in MECs and McA-RH7777 cells. To our surprise, we found that rAAV-HGFK1 exerted no effect on HGF-stimulated cell proliferation but dose dependently inhibited EGF-, VEGF-, and bFGF-mediated cell proliferation. At a MOI of 1×10^4, rAAV-HGFK1 produced significant (80%, 29%, and 46%) inhibitions on EGF-, VEGF-, and bFGF-stimulated MEC proliferation, respectively (Fig. 4*A, left*). Similarly, rAAV-HGFK1 (MOI, 1×10^4) inhibited 83%, 31%, and 34% of EGF-, VEGF-, and bFGF-stimulated cell proliferation, respectively, in McA RH7777 cells (Fig. 4*A, right*).

To validate these observations, we used Western blot analysis to further investigate the effect of rAAV-HGFK1 on the activation of various growth factor receptors. We found that EGFR activation was very sensitive to and was nearly completely inhibited by rAAV-HGFK1 (MOI, 1×10^4) treatment. In contrast, the activations of VEGFR 2 (Flk 1) and bFGFR 1 (Flg) were only partly inhibited by this treatment, and that of HGFR (c-Met) was unaffected (Fig. 4*B*). Taken together, these results suggest that rAAV-HGFK1 exerts both antiangiogenic and antitumor cell effects mainly through inhibition of EGF/EGFR signaling pathways.

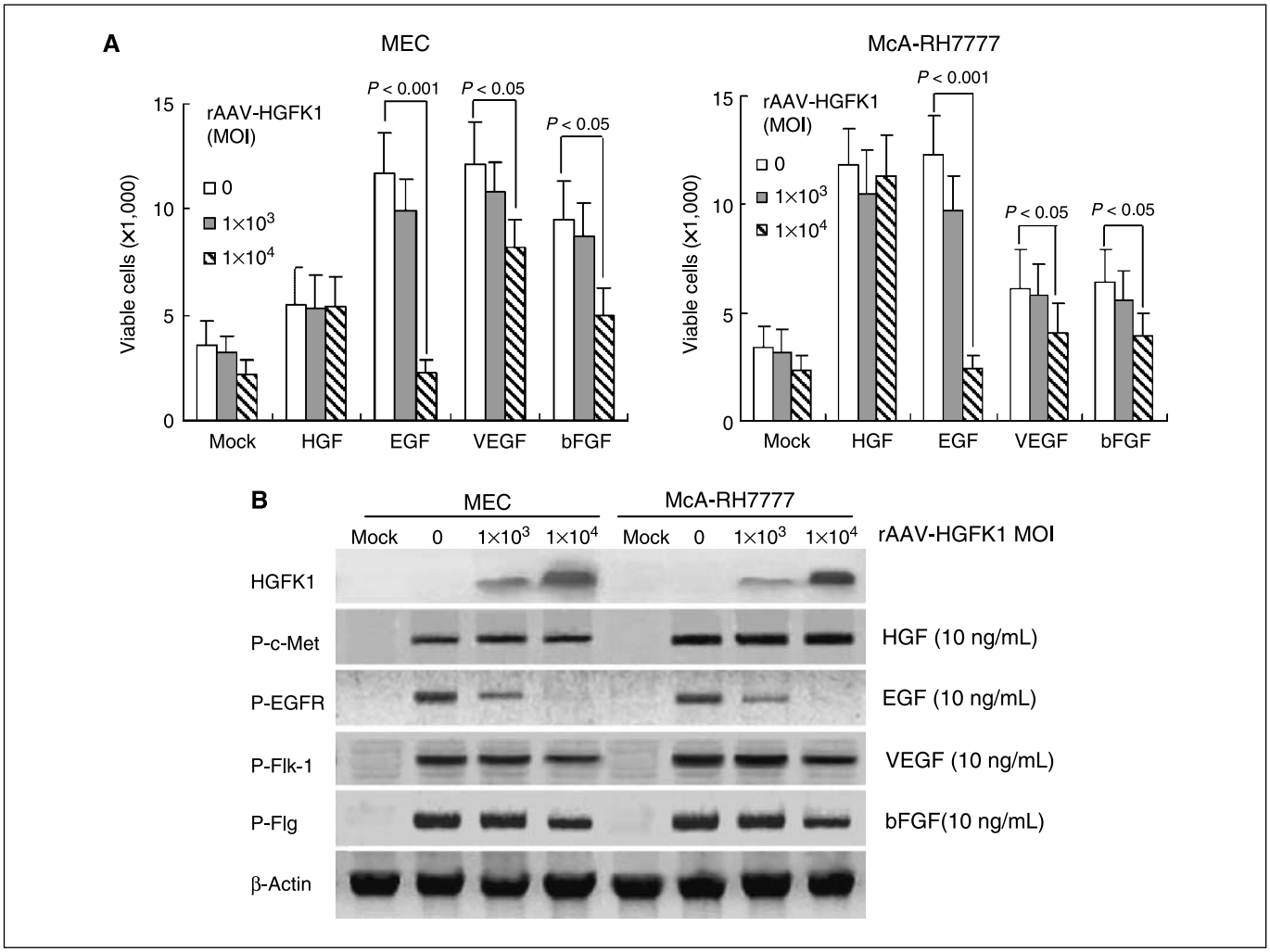

Figure 4. The effects of rAAV-HGFK1 on growth factor–stimulated cell proliferation in MECs and McA-RH7777 cells. Cells were seeded in either (*A*) 96-well or (*B*) 6-well plates, treated with PBS (mock; control) or various concentrations of rAAV-HGFK1 (MOI, 0. 1×10^3 or 1×10^4), incubated in DMEM with 0.5% FBS for 48 h, and then incubated in presence of 10 ng/mL of HGF, EGF, VEGF, or bFGF for an additional 24 h. *A,* viable cells were visualized by trypan blue exclusion method and were counted. *B*, the activation (phosphorylation) of various growth factor receptors (P-c-Met, P-EGFR, P-Flk-1, and P-Flg, respectively) was determined by Western blot analysis using the appropriate antibodies, as described in Materials and Methods.

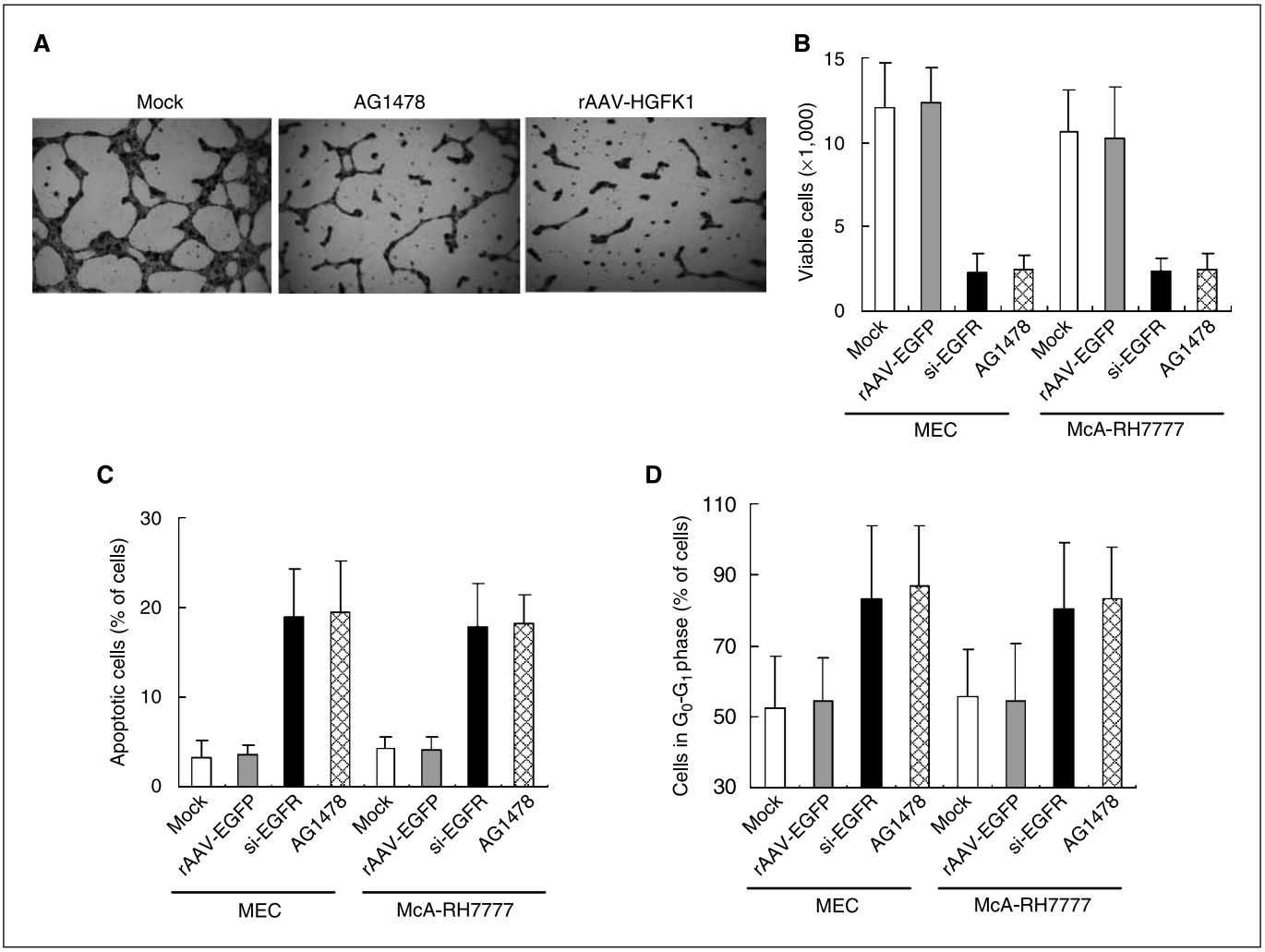

Figure 5. rAAV-HGFK1 decreased angiogenesis, inhibited cell proliferation, induced apoptosis, and triggered G_0-G_1 arrest in MECs and McA-RH7777 cells mainly through EGFR signaling. *A, in vitro* angiogenesis assay. Cells were treated with PBS (*mock*), AG1478 (1 μmol/L), or rAAV-HGFK1 (MOI, 1×10^4), incubated in DMEM with 0.5% FBS for 48 h, and then seeded in ECMatix gel at 4×10^4 cells per well. Capillary structure formation was observed after 5 h. Magnification, ×100. *B* and *C,* MECs and McA-RH7777 cells were seeded in 96-well plates at a density of 2×10^3 cells per well, treated with PBS, rAAV-EGFP (MOI, 1×10^4), si-EGFR (200 pmol), or EGFR-specific–inhibitor AG1478 (1 μmol/L), incubated in DMEM with 0.5% FBS for 48 h, and then stimulated with 10 ng/mL of EGF for an additional 24 h. *B,* viable cells were visualized by trypan blue exclusion, and viable cells per well were counted. *C,* apoptotic cells were stained using the APOPercentage kit, and the percentage of apoptotic cells was determined under an inverted light microscope at ×400 magnification. Five fields were randomly chosen from each sample. *D,* cells were seeded in 6-well plates at a density of 3×10^5 cells per well, treated, incubated, and stimulated as described in *B* and *C*. Flow cytometry was used to determine the percentage of G_0-G_1 cells. The presented data are representative of the results from three independent experiments.

Because, unlike VEGF and bFGF, EGF is generally not considered to be a crucial proangiogenic growth factor, we further tested whether inhibiting EGFR alone could suppress angiogenesis in our system. As shown in Fig. 5*A*, treating MECs with the EGFR-specific inhibitor, AG1478, effectively inhibited the ability of MECs to form capillary-like structures. Consistently, siEGFR and AG1478 abrogated EGF-mediated proproliferation (Fig. 5*B*) and antiapoptotic (Fig. 5*C*) effects in both MECs and McA-RH7777 cells. In addition, si-EGFR and AG1478 induced G_0-G_1 phase arrest of EGF-treated MECs and McA-RH7777 cells (Fig. 5*D*).

rAAV-HGFK1 acts through the EGFR downstream kinases, ERK/JNK, and p38 MAPK, in MECs and McA-RH7777 cells. We investigated the expression and activation of EGFR downstream kinases and found that activation of ERK, p38 MAPK, and JNK was altered by rAAV-HGFK1 treatment in MECs and McA-RH7777 cells, at 48 h posttreatment (Fig. 6*A, left*). A time course study of the activation of EGFR downstream kinases showed that, after inactivation of EGFR, ERK activation was obviously decreased, and the activations of p38 MAPK and JNK were obviously increased at 36 and 48 h after rAAV-HGFK1 treatment. Interestingly, rAAV-HGFK1 had differential effects on the activation of p38 MAPK and JNK in MECs versus McA-RH7777 cells. In MECs, JNK activation was much higher than p38 MAPK activation, whereas in McA-RH7777 cells, p38 MAPK activation was much higher than JNK activation (Fig. 6*A, right*). This differential kinase activation may suggest that JNK and p38 MAPK play unequal roles in HGFK1-mediated effects on MECs and McA-RH7777 cells.

Consistent with this hypothesis, a cell proliferation assay showed that a JNK inhibitor (SP600125) but not a p38 MAPK inhibitor (SB203580) abrogated the antiproliferation effect of rAAV-HGFK1 in MECs. In contrast, the p38 MAPK-kinase inhibitor, but not the JNK inhibitor, abrogated the antiproliferation effect of rAAV-HGFK1 in McA RH7777 cells (Fig. 6*B*). Similarly, apoptotic and cell cycle assays also showed that the JNK inhibitor but not the p38

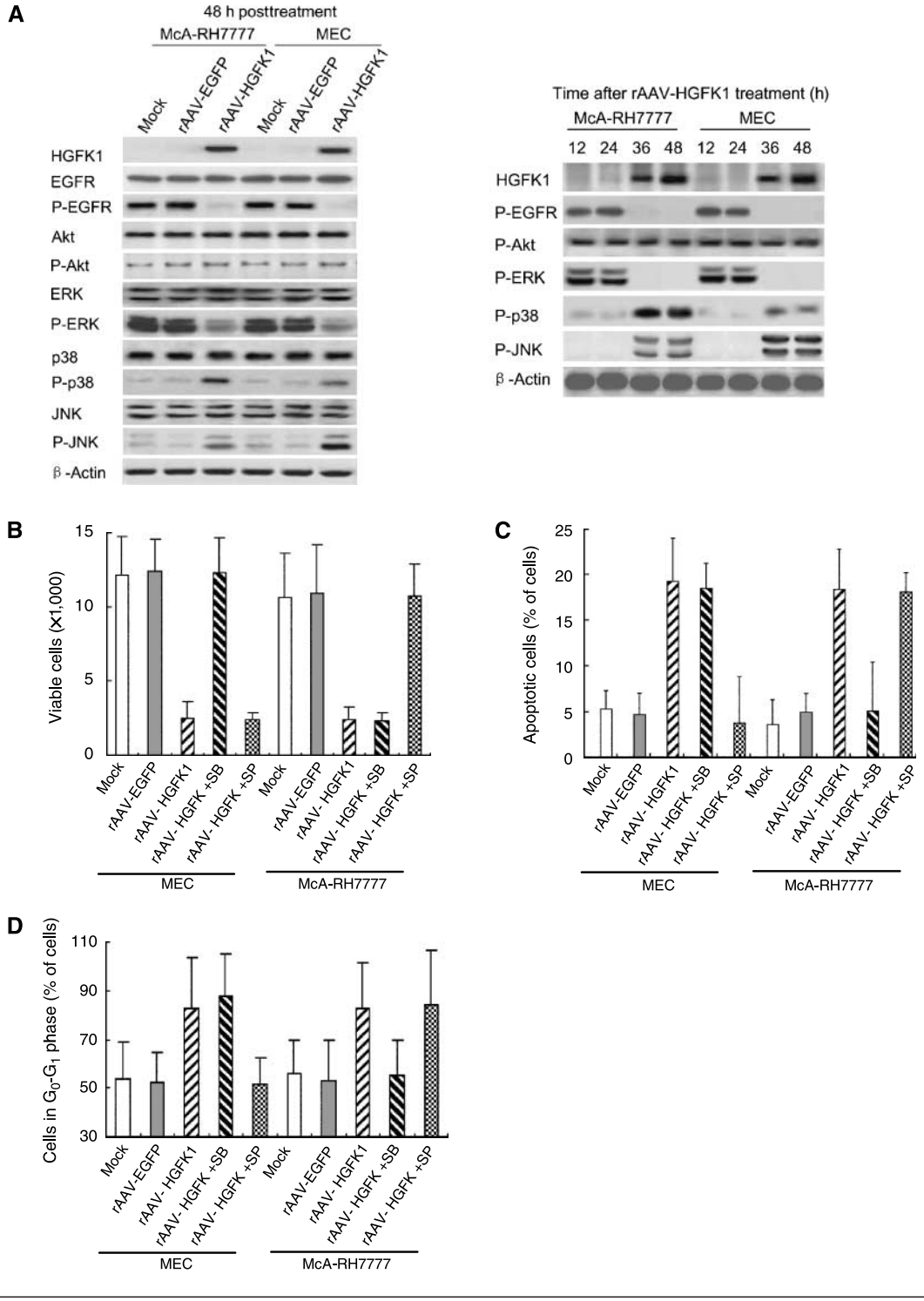

Figure 6. Identification of EGFR and its downstream kinases as the targets of rAAV-HGFK1 in MECs and McA-RH7777 cells. *A,* cells were seeded in 10-cm dishes at a density of 5×10^6 cells per well, treated with PBS (*mock*), rAAV-EGFP, or rAAV-HGFK1 (MOI, 1×10^4), and incubated in DMEM containing 0.5% FBS and 10 ng/mL of EGF for 12, 24, 36, or 48 h. Cells were harvested at each time point, and total proteins were extracted for Western blot analysis. *Left,* the expression of total and phosphorylated EGFR and its downstream kinases, Akt, ERK, p38, and JNK, were determined at 48 h postinfection by Western blot analysis using the appropriate antibodies. *Right,* time-dependent activation of EGFR and its downstream kinases. *B, C,* and *D,* treatment with the p38-specific inhibitor, SB203580 (*SB*), and the JNK-specific inhibitor, SP600125 (*SP*), abrogated the effects of rAAV-HGKF1 on MECs and McA-RH7777 cells. Cells were seeded in 96-well plates at a density of 2×10^3 cells per well, treated with PBS, rAAV-EGFP, rAAV-HGFK1, rAAV-HGFK1+SB, or rAAV-HGFK1+SP, incubated in DMEM with 0.5% FBS for 48 h, and then incubated in DMEM with 0.5% FBS in the presence of 10 ng/mL of EGF for an additional 24 h. *B,* viable cells were identified by trypan blue exclusion, and the number of viable cells per well was counted. *C*, apoptotic cells were stained using the APOPercentage kit, and the percentage of apoptotic cells was determined (magnification, ×400). Five fields were randomly chosen for each sample. *D,* flow cytometry was used to assess the percentage of G_0-G_1 cells. The presented data are representative of the results from three independent experiments.

MAPK kinase inhibitor abolished rAAV-HGFK1–induced apoptosis and G_0-G_1 phase arrest in MECs, whereas the opposite effect was seen in McA-RH7777 cells (Figs. 6*C* and *D*).

Discussion

In the present study, we investigated the *in vivo* therapeutic efficacy of rAAV-HGFK1 in an immunocompetent rat model of orthotopic HCC. We further elucidated the molecular mechanisms of rAAV-HGFK1 *in vitro* in both MECs and tumor cells. Our data showed that rAAV-HGFK1 produced sustained HGFK1 expression *in vivo*, inhibited tumor growth and metastasis, and significantly prolonged the survival time of HCC-bearing rats.The AAV vector system has several advantages as a gene delivery scheme, including long-term transgene expression (22, 29), and low pathogenicity and immunogenicity (30, 31). The present study showed that expression of HGFK1 remained detectable at 120 days after administration of rAAV-HGFK1. Such sustained expression of a therapeutic molecule is especially important for the treatment of cancer by antiangiogenic approaches. Furthermore, we did not observe any toxicity, even after administration of high doses of rAAV-HGFK1, as evaluated in terms of liver biochemistry variables, enzymes related to heart injury, and histologic manifestation of injury in various types of organs. These results suggest that rAAV-mediated gene therapy with HGFK1 is potentially a safe and effective approach for anticancer treatment.

The rAAV-HGFK1 vector constructed in this study mediated secreted HGFK1 expression. When rAAV-HGFK1 was administrated to rats, HGFK1 was secreted from infected cells into the bloodstream and exerted both antiangiogenic and antitumor cell effects. Plasma levels of HGFK1 were examined at several time points (day 0, 7, 21, 60, and 120) after rAAV-HGFK1 injection; the plasma levels of HGFK1 peaked on day 21 and slowly and gradually declined to 75% of the highest level by day 120 (Supplementary Data 4). However, the median survival time was only 49 days, suggesting that HGFK1 levels should be maintained at close to the highest point achieved in this study to achieve therapeutic effects. Therefore, future studies should perhaps involve readministration of rAAV-HGFK1 after day 21 or perhaps administration of a higher initial dose. Although portal vein injection is one choice for drug administration during clinical trials, most studies involve i.v. injection. A previous study showed that i.v. injection of rAAV induces high expression of the delivered gene in both plasma and liver (32), suggesting that i.v. injection could be a suitable route for rAAV-HGFK1 administration. In addition, intratumoral injection could be replaced with injection through hepatic artery catheterization.

We further showed that rAAV-HGFK1 exhibited both antiangiogenic and antitumor cell effects, as rAAV-HGFK1 treatment inhibited the proliferation of both MECs and tumor cells, and induced cell apoptosis. The antiproliferation effect of HGFK1 might be due to G_0-G_1 phase arrest and down-regulation of cyclins and CDKs, whereas its proapoptotic effect was supported by the increased cleavages of caspases 3 and 9. To explore the molecular mechanism of HGFK1-mediated antiangiogenic and antitumor cell effects, we investigated the effect of rAAV-HGFK1 on growth receptor phosphorylation in both MECs and tumor cells. Unexpectedly, rAAV-HGFK1 did not affect HGF-induced cell proliferation and phosphorylation of c-Met. However, rAAV-HGFK1 treatment significantly inhibited EGF-induced EGFR activation. More modest inhibitions of VEGF-induced Flk-1 activation and bFGF-induced Flg activation were also observed in MECs and tumor cells, suggesting that rAAV-HGFK1 exhibits its dual antiangiogenic and antitumor cell effects mainly through EGF/EGFR signaling and partly through the VEGF/VEGFR and bFGF/Flg signaling pathways. Here, we focused primarily on the EGF/EGFR-mediated effects of rAAV-HGFK1. We will explore the related roles of VEGF/Flk-1 and bFGF/Flg signaling in a future study.Although most of the current antiangiogenic drugs are thought to work by inhibiting the synthesis of VEGF by tumor cells, a recent study proposed that these drugs may directly target the endothelium (33). In our study, we found that rAAV-HGFK1, si-EGFR, and the EGFR-specific inhibitor, AG1478, directly inhibited the angiogenic activities of MECs. Consistently, they also inhibited cell proliferation and induced apoptosis and G_0-G_1 phase arrest of both endothelial and tumor cells. Western blot analysis showed that parallel to the decreased phosphorylation of EGFR, rAAV-HGFK1 treatment decreased P-ERK and significantly enhanced P-p38 and P-JNK. These results suggest that rAAV-HGFK1 exerts its effects via multiple signaling molecules, including EGFR, ERK, p38 MAPK, and JNK. We further showed that rAAV-HGFK1 acts via differential EGFR downstream pathways in MECs versus the tested tumor cell line.

In conclusion, the present study showed that rAAV-HGFK1 could mediate sustained HGFK1 expression in both tumor and endothelial cells. Long-term expression of HGFK1 exhibited potent proapoptotic effects on both tumor and endothelial cells, and these proapoptotic effects were dependent mainly on the EGF/EGFR signaling pathway. We found that rAAV-HGFK1–mediated gene therapy significantly prolonged the survival of HCC-bearing rats and exhibited no obvious side effects *in vivo*, even when given at a high dose. Because there is no proven effective systemic therapy for HCC at this time, rAAV-HGFK1 would seem to warrant further investigation, with an eye toward future clinical trials.

Acknowledgments

Received 6/5/2007; revised 9/25/2007; accepted 11/7/2007.

Grant support: Innovation and Technology Commission of the Hong Kong Special Administrative Region, China (ITS/084/03) and RGC (HKU7705/07M).

The costs of publication of this article were defrayed in part by the payment of page charges. This article must therefore be hereby marked *advertisement* in accordance with 18 U.S.C. Section 1734 solely to indicate this fact.

We thank Dr. Samuel Sai-Ming Ng, Wing Sze Leung, and Wayne D. Hsueh for critical reading and editing of the manuscript.

References

1. Folkman J. Angiogenesis in cancer, vascular, rheumatoid and other disease. Nat Med 1995;1:27–32.
2. Hanahan D, Folkman J. Patterns and emerging mechanisms of the angiogenic switch during tumorigenesis. Cell 1996;86:353–64.
3. Kerbel R, Folkman J. Clinical translation of angiogenesis inhibitors. Nat Rev Cancer 2002;2:727–39.
4. Carmeliet P. Angiogenesis in life, disease and medicine. Nature 2005;438:932–8.
5. Jubb AM, Oates AJ, Holden S, Koeppen H. Predicting benefit from anti-angiogenic agents in malignancy. Nat Rev Cancer 2006;6:626–35.
6. Chavakis T, Athanasopoulos A, Rhee JS, et al. Angiostatin is a novel anti-inflammatory factor by inhibiting leukocyte recruitment. Blood 2005;105:1036–43.
7. Veitonmaki N, Cao R, Wu LH, et al. Endothelial cell surface ATP synthase-triggered caspase-apoptotic pathway is essential for k1-5-induced antiangiogenesis. Cancer Res 2004;64:3679–86.
8. Kuba K, Matsumoto K, Date K, Shimura H, Tanaka M, Nakamura T. HGF/NK4, a four-kringle antagonist of hepatocyte growth factor, is an angiogenesis inhibitor that suppresses tumor growth and metastasis in mice. Cancer Res 2000;60:6737–43.

9. Kazuhiko D, Kunio M, Hideo S, Masao T, Toshikazu N. HGF/NK4 is a specific antagonist for pleiotrophic actions of hepatocyte growth factor. FEBS Lett 1997;420:1–6.

10. Yu AS, Keeffe EB. Management of hepatocellular carcinoma. Rev Gastroenterol Disord 2003;3:8–24.

11. Llovet JM, Burroughs A, Bruix J. Hepatocellular carcinoma. Lancet 2003;362:1907–17.

12. Bruix J, Llovet JM. Hepatocellular carcinoma: is surveillance cost effective? Gut 2001;48:149–50.

13. Johnson PJ. Hepatocellular carcinoma: is current therapy really altering outcome? Gut 2002;51:459–62.

14. Zhu AX, Blaszkowsky LS, Hale KE, et al. Phase II study of gemcitabine and oxaliplatin in combination with bevacizumab in patients with advanced hepatocellular carcinoma. J Clin Oncol 2006;24:1898–903.

15. Llovet JM, Chen Y, Wurmbach E, etal. A molecular signature to discriminate dysplastic nodules from early hepatocellular carcinoma in HCV cirrhosis. Gastroenterology 2006;131:1758–67.

16. Vejchapipat P, Tangkijvanich P, Theamboonlers A, et al. Association between plasma hepatocyte growth factor and survival in untreated hepatocellular carcinoma. J Gastroenterol 2004;39:1182–8.

17. Xin L, Xu R, Zhang Q, Li TP, Gan RB. Kringle 1 of human hepatocyte growth factor inhibits bovine aortic endothelial cell proliferation stimulated by basic fibroblast growth factor and causes cell apoptosis. Biochem Biophys Res Commun 2000;277:186–90.

18. Hoffmann S, Wunderlich A, Celik I, et al. Paneling human thyroid cancer cell lines for candidate proteins for targeted anti-angiogenic therapy. J Cell Biochem 2006;98:954–65.

19. Kurup A, Lin CW, Murry DJ, et al. Recombinant human angiostatin (rhAngiostatin) in combination with paclitaxel and carboplatin in patients with advanced non-small-cell lung cancer: a phase II study from Indiana University. Ann Oncol 2006;17:97–103.

20. Samulski RJ, Chang LS, Shenk T. Helper-free stocks of recombinant adeno-associatd viruses: normal integration does not require viral gene expression. J Virol 1989; 63:3822–8.

21. Liu CC, Shen Z, Kung HF, Lin CM. Cancer gene therapy targeting angiogenesis: an updated review. World J Gastroenterol 2006;12:6941–8.

22. Ponnazhagan S, Mahendra G, Kumar S, et al. Adeno-associated virus 2-mediated antiangiogenic cancer gene therapy: long-term efficacy of a vector encoding angiostatin and endostatin over vectors encoding a single factor. Cancer Res 2004;64:1781–7.

23. Merten OW, Geny-Fiamma C, Douar AM. Current issues in adeno-associated viral vector production. Gene Ther 2005;Suppl 1:S51–61.

24. Chen Y, Luk KD, Cheung KM, et al. Gene therapy for bone formation using adeno associated viral bone morphogenetic protein 2 vectors. Gene Ther 2003;10: 1345–53.

25. Grimm D, Kern A, Rittner K, Kleinschmidt JA. Novel tools for production and purification of recombinant adenoassociated virus vectors. Hum Gene Ther 1998;9: 2745–60.

26. Yang ZF, Ho DW, Lam CT, et al. Identification of brain-derived neurotrophic factor as a novel functional protein in hepatocellular carcinoma. Cancer Res 2005; 65:219–25.

27. Lum CT, Yang ZF, Li HY, et al. Gold(III) compound is a novel chemocytotoxic agent for hepatocellular carcinoma. Int J Cancer 2006;118:1527–38.

28. Soumaoro T, Uetake H, Higuchi T, et al. Cyclooxygenase-2 expression a significant prognostic indicator for patients with colorectal cancer labile. Clin Cancer Res 2004;10:8465–71.

29. Yang ZF, Wu XB, Tsui TY, et al. Recombinant adeno-associated virus vector: Is it ideal for gene delivery in liver transplantation? Liver Transpl 2003;9:411–20.

30. Rabinowitz JE, Samulski J. Adeno-associated virus expression systems for gene transfer. Curr Opin Biotechnol 1998;9:470–5.

31. Subramanian IV, Bui Nguyen TM, Truskinovsky AM, et al. Adeno-associated virus-mediated delivery of a mutant endostatin in combination with carboplatin treatment inhibits orthotopic growth of ovarian cancer and improves long-term survival. Cancer Res 2006;66: 4319–28.

32. Mingozzi F, Schüttrumpf J, Arruda VR, et al. Improved hepatic gene transfer by using an adeno-associated virus serotype 5 vector. J Virol 2002;76:10497–502.

33. Baker CH, Kedar D, McCarty MF, et al. Blockade of epidermal growth factor receptor signaling on tumor cells and tumor-associated endothelial cells for therapy of human carcinomas. Am J Pathol 2002;161:929–38.